Applying the Dynamic Absorber Theory for the Control of FPSOs Rolling Motion

Arhur Curty Saad, *PETROBRAS*
Antonio Carlos Fernandes, *COPPE/UFRJ*
Paulo de Tarso T. Esperança, *COPPE/UFRJ*
Joel Sena Sales Jr., *COPPE/UFRJ*

ABSTRACT

The FPSOs are a type of offshore platforms that are directional in nature. It has been found that there is a possibility, in certain cases, that a rolling resonant wave may reach some stationary FPSOs and consequently, a very high response may be obtained. Sometimes it is not possible to use large bilge keel and the alternative is to consider the use of other devices such as stabilizing tanks and U-tubes. Faced with this problem, in order to organize the subject analyses, the work decided to consider the utilization of a dynamic absorber to control the rolling motion. For that, a passive mass was placed on board and the fully three dimensional and non-linear model is formulated. Subsequently, a careful linearization is made for the purpose of identifying the commanding variables such as the mass, the position above the keel, the damping, the dynamic absorber natural frequencies, etc. After that, several parametric studies have been performed, identifying the range of applicability of the variables. Based on these preliminary studies, the work describes the use of reduced model tests showing the usefulness of the theory in practice. The tests have been made in a deepwater ocean basin.

Keywords: *Roll Motion of FPSO, Roll Control, Dynamic Absorber*

1. INTRODUCTION

Presently, the FPSO (Floating Production Storage and Offloading) is the main type of platform option for hydrocarbons production, offshore Brazil.

It turns out that for several of these platforms already installed, large roll amplitude has been observed. Is has becoming clear that this is due to the closeness of the predominant “swell” period and the FPSO natural period, that is it is a resonant or near resonant condition. It is possible to reduce this motion by the so-called “pull-back” operation, by moving the heading away from the 90 degrees with respect to the swell direction. However, this is a costly operation and solution that does not need docking is needed. The use of devices such as U-tubes stabilizing tanks must be considered. Hence the present work decided to investigate these alternatives and as a first step, a direct and clear study for the applicability of the Dynamic Absorber (DA) Theory has been pursued. Both a complete mathematical non-linear formulation and experimental methods has been conducted. The simpler way is to place a linear mass-spring-dashpot system on board and then treat the problem initially in a fully non-linear way. Subsequently a linearization is performed arriving to a practical method for preliminary design and parametric study.

For validation, a complete set of experiments in the model basin were made, confirming practically the mathematical model and the applicability of the Dynamic Absorber

Theory.

2. THEORETICAL MODEL WITH SIX DEGREES OF FREEDOM

2.1 General Equations

Figure 1 contains the coordinate system.

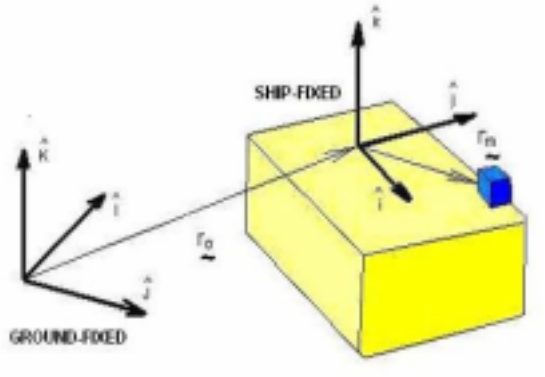

Figure 1. Reference systems and mass on board.

Based on the definitions in Figure 1, it is possible to show that (Saad, 2005) the equations of motion may be written by (1).

$$\vec{F}_{SHIP} = m.\vec{g} - m.\overrightarrow{A_m} \tag{1}$$

where $\vec{g}$ in Cartesian coordinates is given by:

$$\vec{g} = (g_x, g_y, g_z) \tag{2}$$

and

$$\begin{aligned}
&\vec{F}_{SHIP} = \\
&m\dot{\vec{i}}(g_x - u' - qw + rv + 2ry' - q'z_m + r'y \\
&- pqy + q^2x_m + r^2x_m - prz_m) + \\
&m\vec{j}(g_y - v' - ru + pw - y'' - r'x_m + p'z_m \\
&- rqz_m + r^2y + p^2y - pqx_m) + \\
&m\vec{k}(g_z - w' - pv + qu - 2.py' - p'y \\
&+ q'x_m - prx_m + p^2z_m + q^2z_m - rqy)
\end{aligned} \tag{3}$$

While for the moment, since

$$\vec{M}_{SHIP} = \overrightarrow{r_m} \times \vec{F}_{SHIP} \tag{4}$$

the following is true

$$\begin{aligned}
&\vec{M}_{SHIP} = \\
&m\dot{\vec{i}}[y(g_z - w' - pv + qu - 2py' - p'y \\
&+ q'x_m - prx_m + p^2z_m + q^2z_m - rqy) \\
&- z_m(g_y - v' - ru + pw - y'' - r'x_m + p'z \\
&{}_m - rqz_m + r^2y + p^2y - pqx_m)] + \\
&m\vec{j}[z_m(g_x - u' - qw + rv + 2ry' - q'z_m \\
&+ r'y - pqy + q^2x_m + r^2x_m - prz_m) \\
&- x_m(g_z - w' - pv + qu - 2py' - p'y \\
&+ q'x_m - prx_m + p^2z_m + q^2z_m - rqy)] + \\
&m\vec{k}[x_m(g_y - v' - ru + pw - y'' - r'x_m \\
&+ p'z_m - rqz_m + r^2y + p^2y - pqx_m) \\
&- y(g_x - u' - qw + rv + 2ry' - q'z_m \\
&+ r'y - pqy + q^2x_m + r^2x_m - prz_m)]
\end{aligned} \tag{5}$$

The equations above correct the some typographical mistakes in (Treakle et al., 1999).

2.2 Two Degrees of Freedom; Linearization; Frequency Domain

For small displacement a consistent linearization has been performed by Saad (2005). The result in matrix form is given by (6).

$$\begin{aligned}
&\begin{bmatrix} I_{xx} + A_{44} + m.z_m^{\,2} & -m.z_m \\ -m.z_m & m \end{bmatrix} \begin{bmatrix} \eta_4'' \\ y'' \end{bmatrix} \\
&+ \begin{bmatrix} B_{44} & 0 \\ 0 & c \end{bmatrix} \begin{bmatrix} \eta_4' \\ y' \end{bmatrix} \\
&+ \begin{bmatrix} C_{44} - m.g.z_m & -m.g \\ -m.g & k \end{bmatrix} \begin{bmatrix} \eta_4 \\ y \end{bmatrix} = \begin{bmatrix} M_{wave} \\ 0 \end{bmatrix}
\end{aligned} \tag{6}$$

where M_{wave} is the wave exciting moment.

In the frequency domain these equations

may be written as in Eq. (7)

$$\begin{bmatrix} -\omega^2.(I_{xx}+A_{44}+m.z_m^{\,2})+i.\omega.B_{44}+C_{44}-m.g.z_m & \omega^2.m.z_m-m.g \\ \omega^2.m.z_m-m.g & k-\omega^2.m+i.\omega.c \end{bmatrix}\begin{bmatrix} I_4 \\ Y \end{bmatrix} = \begin{bmatrix} M \\ 0 \end{bmatrix} \quad (7)$$

The ship inclination amplitude (I4) and the mass displacement amplitude (Y) may then be writen respectively as in Eq. (8) and Eq. (9).

$$I_4 = \frac{[(-k-i.c.\omega+m^2.k).M]}{\begin{aligned}&[-C_{44}.k-g.z_m.m.k-i.g.z_m.m.c.\omega\\&-i.C_{44}.c.\omega+C_{44}.m.\omega^2+B_{44}.\omega^2.c\\&+i.B_{44}.\omega^3.m+\omega^2.I_{44}.k+i.\omega^3.I_{44}.c\\&-\omega^4.I_{44}.m+\omega^2.A_{44}.k+i.\omega^3.A_{44}.c\\&-\omega^4.A_{44}.m+\omega^2.m.z_m^{\,2}.k\\&+i.\omega^3.m.z_m^{\,2}.c+m^2.g^2-\omega^2.g.z_m.m^2\\&-i.\omega.B_{44}.k]\end{aligned}} \quad (8)$$

$$Y = \frac{[(g-z_m^{\,2}.\omega).m.M]}{\begin{aligned}&[-C_{44}.k-g.z_m.m.k-i.g.z_m.m.c.\omega-i.C_{44}.c.\omega+\\&C_{44}.m.\omega^2+B_{44}.\omega^2.c+i.B_{44}.\omega^3.m+\omega^2.I_{44}.k+\\&i.\omega^3.I_{44}.c-\omega^4.I_{44}.m+\omega^2.A_{44}.k+i.\omega^3.A_{44}.c-\\&\omega^4.A_{44}.m+\omega^2.m.z_m^{\,2}.k+i.\omega^3.m.z_m^{\,2}.c+m^2.g^2-\\&\omega^2.g.z_m.m^2-i.\omega.B_{44}.k]\end{aligned}} \quad (9)$$

The eigenvalues follow easily and are given in Eq. (10).

$$\omega_{1,2} = \sqrt{\frac{\begin{aligned}&[k.(I_{xx}+A_{44}+m.z_m^{\,2})+m.(C_{44}+m.g.z_m)]\pm\\&\{[k.(I_{xx}+A_{44}+m.z_m^{\,2})+\\&m.(C_{44}+m.g.z_m)]^2-\\&4[m.(I_{xx}+A_{44})].[k.(C_{44}-m.g.z_m)-m^2.g^2]\}^{1/2}\end{aligned}}{2.[m.(I_{xx}+A_{44})]}} \quad (10)$$

3. EXPERIMENTAL VALIDATION

Before using the frequency domain equations the work decided to seek its comprehensibleness with model testing. The model chosen for this study is the one depicted in Figure 2. It corresponds to a 1:75 VLCC parallel middle body slice.

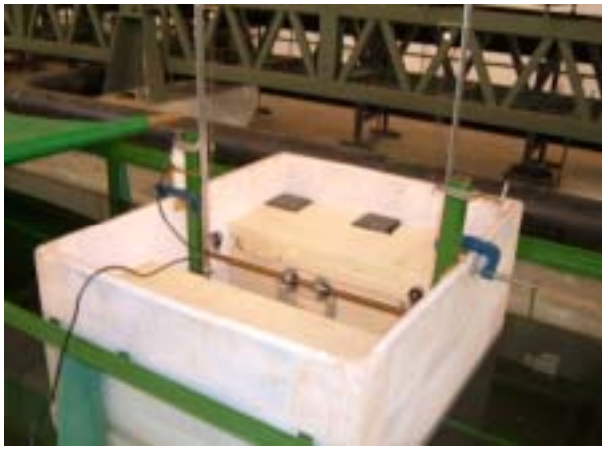

Figure 2 – Model Scale (parallel middle body slice with DA system).; assembly at the LOC flume.

Two tests were made: the decaying tests and the tests with incident waves (regular and random). Some tests were made in a flume in the LOC/COPPE/UFRJ (Laboratório de Ondas e Correntes – Waves and Currents Laboratory at COPPE/UFRJ). However, the majority of the tests were made in LabOceano (Laboratório de Tecnologia Oceânica – Ocean Technology Laboraory at COPPE/UFRJ).

The characteristics of the model are given in Table 1. For assembly details see (Saad 2005).

Table 1. Model characteristics

	Scale	Real
Length	0,905 m	67,88 m
breadth	0,73 m	54,75 m
depth	0,45 m	33,75 m
Draft	0,096 m	7,20 m
Displacement	61,47 Kg	25932,66 Ton
KG	0,24 m	18,00 m
Tn	1,37 s	11,86 s

3.1 Decaying Tests

The main objective of this test is to confirm the designed natural period without the DA in operation. A typical time series from this test is shown in Figure 3. The natural period is 1.37 s. Three DA were tested (see Saad (2005)). One result for the DA mass 3,355 Kg and DA spring stiffness is 70.1 (N/m) (called by Saad

(2005)) is given in Figure 4. The effectiveness of the DA is quite impressive.

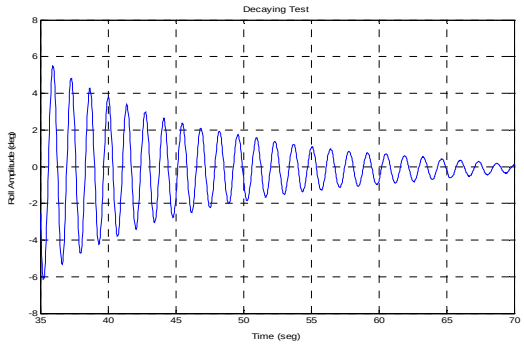

Figure 3 –Decaying tests for a VLCC parallel middle body slice.

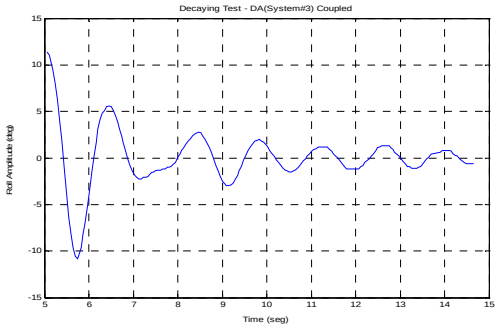

Figure 4 –Decaying tests for a VLCC parallel middle body slice with the DA (System#3) in operation.

3.2 Incident Waves Tests Comparisons with the 1 DOF Frequency Domain Model

Again at first the comparison has been made without the DA in operation. Typical result is shown in Figure 5 using an experimental random wave technique to identify RAO. This is to show that the 2 DOF frequency domain model for this case is enough as expected. In Figure 6 the same testing were performed with the DA (Sytem#3) in operation.

Again the results are close enough for this extremely simplified theoretical model. In Figure 6 it is shown the prediction and measured result for the lateral displacement of the DA mass. Several other results are presented in Saad (2005).

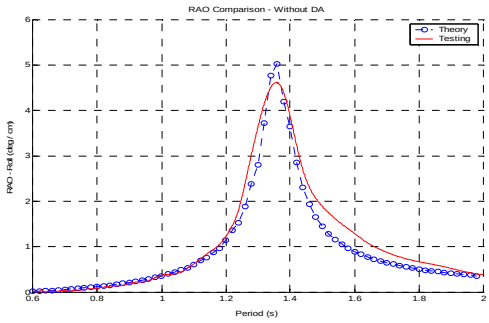

Figure 5 – RAO obtained from random wave testing; model without the DA; 2DOF frequency domain theory.

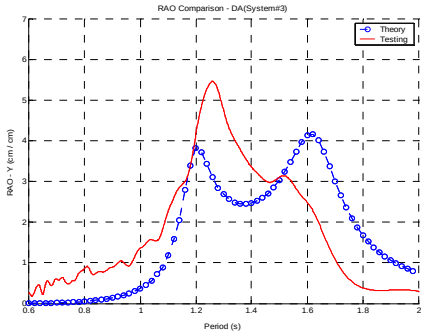

Figure 6. –Comparison for the lateral displacement (Systema#3); theory and experiment

3.3 Conclusion from the comparisons'

The main conclusion from the comparisons between the model testing and the simplified 2 DOF (one DOF for the roll angle and one DOF for the lateral DA mass displacement) is that the order of magnitude is reached for both. In fact it is rewarding to observe and measure the effectiveness of the DA during the model test at the LOC and at the LabOceano. However several other conclusions will be addressed later what includes the improvement of the model testing. However, the work decided to go on with a parametric study with the theoretical model.

4. PARAMETRIC RESULTS FROM THE SIMPLIFIED THEORETICAL MODEL

Due to the simplicity of the mathematical model equations several results may be obtained. As in the model testing, the work decided to tackle a floating body made from VLCC parallel middle body slice. This is shown in Figure 1 and the potential theory panels are shown in Figure 7.

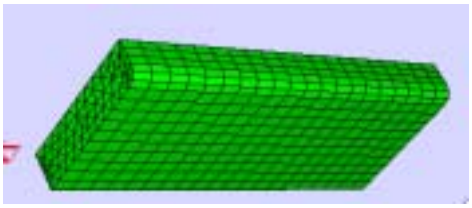

Figure 7. Panel definition for a floating body made with a VLCC main section; Input panels for a Frequency Domain code.

4.1 Dynamic Absorber Characteristics

The parametric investigation refers to the systematic variation of the parameters of the DA. A datum DA is presented in Table 2 and the following parameters have been systematically changed:

- the on board body mass,
- the vertical position of its center of gravity,
- the natural period and the damping.

Table 2. Characteristics of a datum dynamic absorber

Mas	1.842 Kg
Stiffness	39,1 N/m
Damp.	1,69 kg/s
T	1,37s

The responses from the parametric study are shown next. Firstly, in Figure 8, the RAO response for the case without and with the datum dynamic absorber. The effect is indeed dramatic.

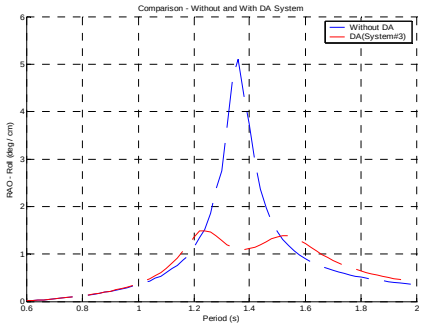

Figure 8. RAO response without and with the datum dynamic absorber.

In Figure 9, it is shown the effect of the mass as a percentage from the floating body mass. The stiffness has been changed in order to keep the same dynamic absorber natural period. It is shown that from 2% the response becomes bimodal. From 3% to 6% there are no significant differences.

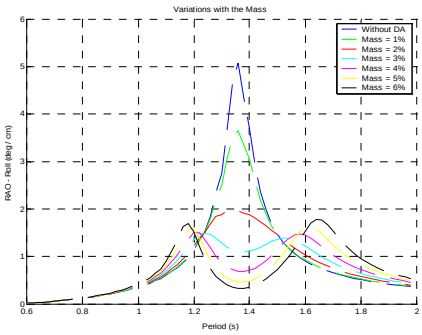

Figure 9. Variations with the DA mass.

In Figure 10, the influence of the vertical position of the dynamic absorber plane is shown both above and below the CG of the floating body expressed as ration of the beam.

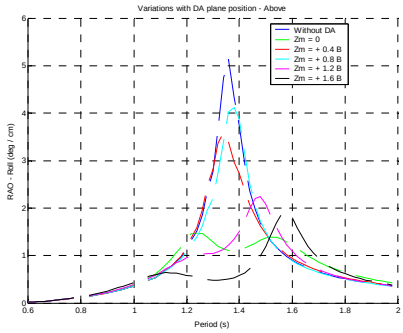

Figure 10. DA plane position above the floating body CG

Note that from heights between 0.4 B e 0.8 B, the RAO is larger; this trend changes for the 1.2 B e 1.6 B cases.

In Figure 11, the result of placing the DA plane below the FB CG is shown. At first sight, this is a surprising result due to the clear amplitude reduction much better than the cases above the CG (Figure 10). In fact, the reduction is approximately proportional to the vertical distance. However, note that in Eq. (8) (for I4) there is a –zm term in the denominator that leads to a smaller response for the negative case! One may probably anticipate an important conclusion that a stabilizer below deck is better placed below CG!

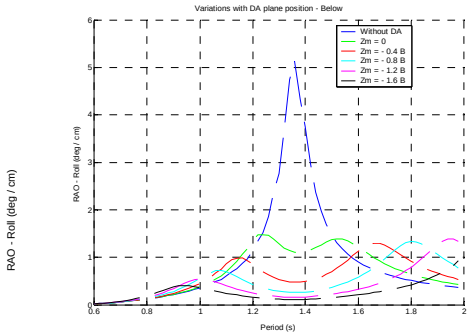

Figure 11. Dynamic absorber plane below the floating body CG.

In Figure 12 and 13, the work shows the influence of the variations of the natural period. The objective is to understand the importance of the tuning. In Figure 12, one has results for periods above the datum DA and in Figure 13, for the period below it.

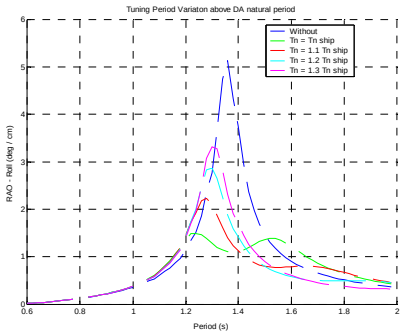

Figure 12. Tuning period variation above the datum DA natural period.

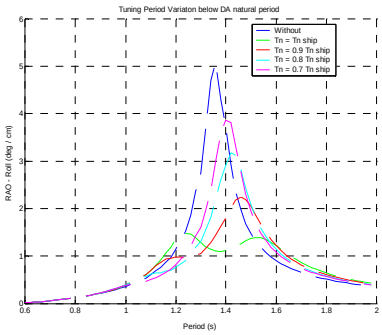

Figure 13. Tuning period variation below the datum DA natural period.

For both cases (Figure 12 and 13) there is no bi-modal responses when the tuning is absent.

Finally in Figure 14, the influence of the damping is shown. The role of the damping is to decrease the twin peaks height and at same time increase the trough from zero (zero damping case). It is interesting to realize that these results comply with the optimum damping concept as suggested by Den Hartog (1985). The latter is such that the difference between the two peaks and the trough is as smaller as possible. From Figure 14 one may say in this case that the optimum damping is between 10% and 20% of the critical damping. Besides for damping smaller than 5% from the critical damping, the bi-modal character is maintained. For cases above 20% from the critical damping, there is one peak with smaller RAO.

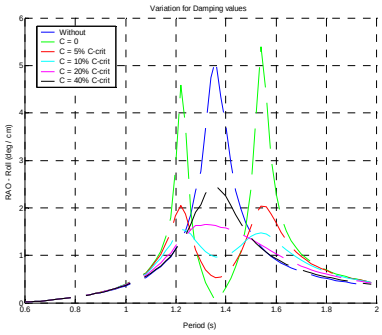

Figure 14. Consequences of the various damping values.

5. CONCLUSIONS

The work has reviewed the time domain equations for the 9 DOF (6 DOF for the ship and 3 DOF DA mass displacement). This correct some typographical errors in the literature.

The linearized model yields results with the same order of magnitude of the model tests. This model can be improved easily with a 3 DOF rolling problem (3 DOFs – sway, heave an roll - and 1 DOF for the DA mass) in order to verify if the motion coupling is really important.

The model testing confirmed the effectiveness of having a DA on board to control the roll response.

Another improvement could be made with a better estimation of the damping coefficients.

It is important to call the attention for the vertical position of the DA operational plane. The work clearly shows that the lower positions are more efficient.

6. ACKNOWLEDMENTS

We are grateful to PETROBRAS for allowing the first author to pursue its master degree. We thank CNPq (Brazilian National Research Council) and finally the LabOceano and LOC from COPPE/UFRJ. The model testing of the work has been considered to be academically motivated and therefore was considered complimentary.

7. REFERENCES

Hartog, J. P. D., 1985, “Mechanical Vibrations”, Dover Books on Engineering.

Saad, A. C., 2005, “Aplicação da Teoria do Absorvedor Dinâmico de Vibração na Redução Do Balanço Transversal em Plataformas Tipo FPSO”, M.Sc. Thesis, COPPE/UFRJ, Federal University of Rio de Janeiro, Brazil (in Portuguese).

Treakle, T. W., 1998, “A Time Domain Numerical Study of a Passive and Active Anti-Roll Tanks to Reduce Ship Motions”, M.Sc. Thesis, Faculty of Virginia Polytechnic Institute and State University, Blacksburg, VA, United States of America.